1
In-situ Synthesis of Polymer Nanocomposites

Vikas Mittal

1.1
Introduction

It was the pioneering work of Toyota researchers toward the development of polymeric nanocomposites in the early 90s [1, 2], in which electrostatically held 1-nm-thick layers of the layered aluminosilicates were dispersed in the polyamide matrix on a nanometer level, which led to an exponential growth in the research in these layered silicate nanocomposites. These nanocomposites were based on the *in-situ* synthesis approach in which monomer or monomer solution was used to swell the filler interlayers followed by polymerization. Subsequently, Giannelis and coworkers [3, 4] also reported the route of melt intercalation for the synthesis of polymer nanocomposites.

Montmorillonite has been the most commonly used layered aluminosilicate in most of the studies on polymer nanocomposites. The general formula of montmorillonites is $M_x(Al_{4-x}Mg_x)Si_8O_{20}(OH)_4$ [5, 6]. Its particles consist of stacks of 1-nm-thick aluminosilicate layers (or platelets) with a regular gap in between (interlayer). Each layer consists of a central Al-octahedral sheet fused to two tetrahedral silicon sheets. In the tetrahedral sheets, silicon is surrounded by four oxygen atoms, whereas in the octahedral sheets, aluminum atom is surrounded by eight oxygen atoms. Isomorphic substitutions of aluminum by magnesium in the octahedral sheet generate negative charges, which are compensated for by alkaline-earth- or hydrated alkali-metal cations. Owing to the low charge density (0.25–0.5 equiv. mol^{-1}) of montmorillonites, a larger area per cation is available on the surface that leads to a lower interlayer spacing in the modified montmorillonite after surface ion exchange with alkyl ammonium ions. On the contrary, the minerals with high charge density (1 equiv. mol^{-1}) like mica have much smaller area per cation and can lead to much higher basal plane spacing after surface modification; however, owing to very strong electrostatic forces present in the interlayers due to the increased number of ions, these minerals do not swell in water and thus do not allow the cation exchange. In contrast, aluminosilicates with medium charge densities of 0.5–0.8 equiv. mol^{-1} like vermiculite offer a potential of partial swelling in water and cation exchange that can lead to much higher basal plane spacing in

In-situ Synthesis of Polymer Nanocomposites, First Edition. Edited by Vikas Mittal.

the modified mineral if optimum ion exchange is achieved. Vaia *et al.* [7] also proposed further insight into the positioning of the surface modification molecules on the surface of the filler based on FTIR experiments. By monitoring frequency shifts of the asymmetric CH_2 stretching and bending vibrations, they found that the intercalated chains exist in states with varying degrees of order. In general, as the interlayer packing density or the chain length decreases (or the temperature increases), the intercalated chains adopt a more disordered, liquid-like structure resulting from an increase in the gauche/trans conformer ratio.

Nanocomposites with a large number of polymer matrices have been synthesized and significant enhancements in the composite properties have been reported. The improvement in the mechanical properties of the nanocomposites is generally reported, though a synergistic enhancement in the other composite properties like gas barrier resistance is also generally achieved. Figure 1.1a demonstrates the decrease in oxygen permeation through the polyurethane, epoxy, and polypropylene nanocomposites as a function of inorganic filler volume fraction [8–10]. Figure 1.1b also shows the improvement in mechanical properties of the polypropylene and polyethylene nanocomposites as a function of filler volume fraction [11–13]. The polypropylene composites have been generated by using two different filler surface modifications containing ammonium and imidazolium ions. The microstructure of the nanocomposites is also ideally classified as unintercalated (phase separated), intercalated, and exfoliated composites. The composite microstructure is classified as exfoliated when the filler platelets are completely delaminated into their primary nanometer scale size and the platelets are far apart from each other so that the periodicity of this platelet arrangement is totally lost. When a single or sometimes more than one extended polymer chain is intercalated into the clay interlayers, but the periodicity of the clay platelets is still intact, such a microstructure is termed as intercalated. On the basis of the interfacial interactions and mode of mixing of the organic and inorganic phases, it is possible that both the phases do not intermix at all and a microcomposite or unintercalated composite is formed. Transmission electron microscopy (TEM) and X-ray diffraction (XRD) are the most commonly used methods to characterize the microstructure of the nanocomposites. Figure 1.2 shows the TEM micrographs depicting the various idealized morphologies of the polymer nanocomposite structures [15]. However, it should be noticed that these classifications of the composite microstructure as exfoliated and intercalated are not very realistic as generally in reality a mixture of different morphologies is present. Figure 1.3 also shows the three idealized morphologies of immiscible, intercalated, and exfoliated composites [16]. The presence or absence of diffraction peaks in the XRD of the composites is used to assess information about the microstructure of the composites. The intensity of the X-ray diffractograms is generally taken as a measure to classify the microstructure as intercalated or exfoliated. However, it should be noticed that the X-ray signal are very qualitative in nature and are strongly influenced by the sample preparation, orientation of the platelets, as well as defects present in the crystal structure of the montmorillonites. Therefore, the classification of the nanocomposite microstructure just based on the intensity can be faulty. Also, the presence

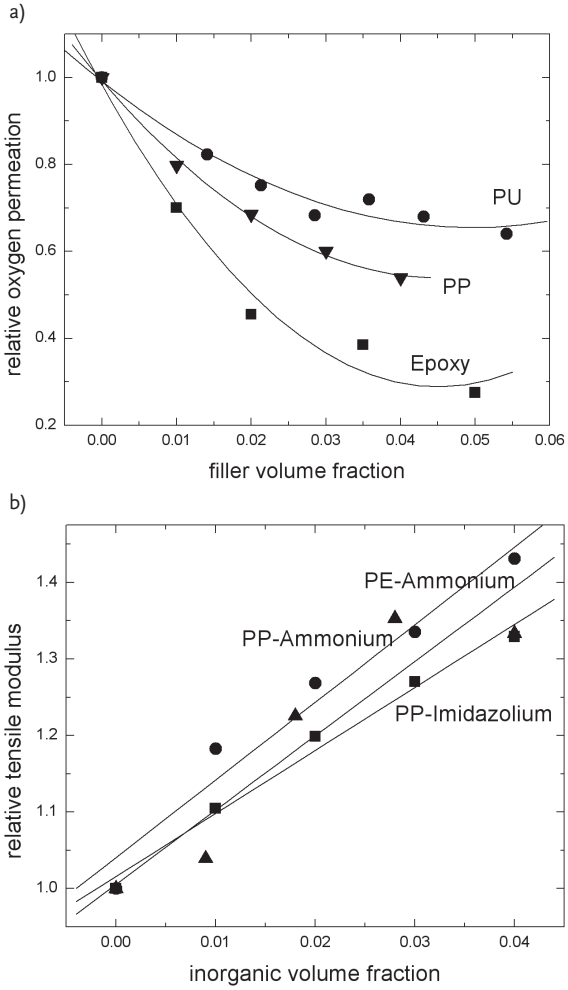

Figure 1.1 (a) Relative oxygen permeation and (b) relative tensile modulus of various polymer nanocomposites as a function of filler volume fraction [8–13]. Reproduced from Ref. [14].

of diffraction signal in the diffractograms of the composite does not mean that 100% of the microstructure is intercalated and it is quite possible to have significant amount of exfoliation present in the composite. Similarly, absence of diffraction signal also does not guarantee the complete exfoliation as small or randomly oriented intercalated platelets may still be present in the composite.

Many factors influence the microstructure and hence the properties of the nanocomposites. The first of such factors is the surface modification of the filler and its interaction with the polymer. The modification is required to make the filler organophilic and to push the filler interlayers apart, thus providing possibilities for polymer intercalation. Table 1.1 details the various kinds of surface

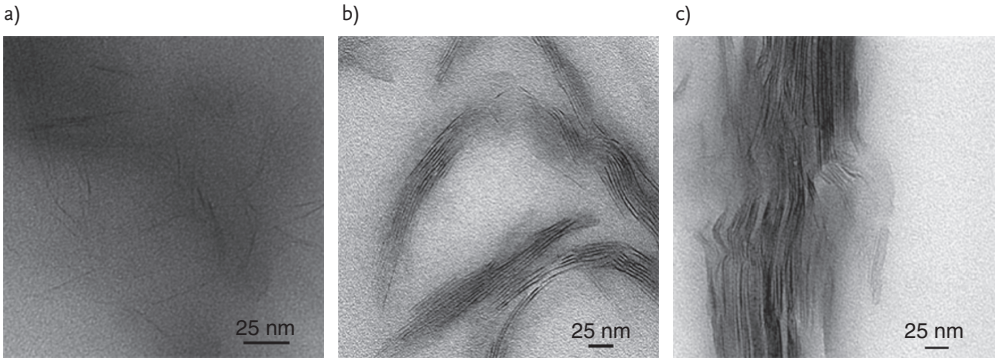

Figure 1.2 TEM micrographs indicating various possible morphologies in the composites as a function of the filler distribution: (a) exfoliated, (b) intercalated, and (c) unintercalated. Reproduced from Ref. [15] with permission from Wiley.

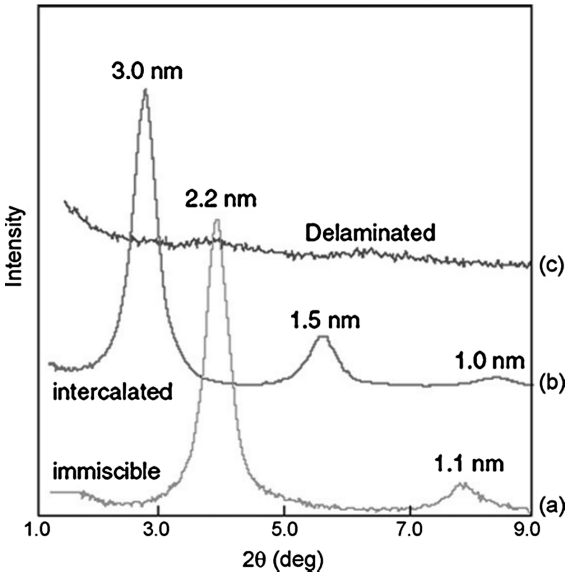

Figure 1.3 XRD patterns of immiscible, intercalated, and exfoliated composites. Reproduced from Ref. [16] with permission from Elsevier.

modifications commonly used to modify the filler surface. The basal plane spacing of the filler resulting after the surface modification is also provided. The modifications differ in many aspects such as chain length, density of the chains in the surface modification molecule, and chemical architecture. The modification molecules have specific interactions with the matrix polymer and these interactions are responsible for the ability of the filler to exfoliate or delaminate in the polymer matrix [8, 9]. Figure 1.4 shows an example of such interplay of interactions between

Table 1.1 Basal plane spacing values of various surface-modified montmorillonites and vermiculites [8–13].

Modification	Substrate, CEC (μ.eq g^{-1})	Basal spacing (nm)
Octadecyltrimethylammonium	Montmorillonite, 880	1.84
Octadecyltrimethylammonium	Montmorillonite, 680	1.82
Octadecyltrimethylammonium	Montmorillonite, 900	1.85
Octadecyltrimethylammonium	Montmorillonite, 1000	2.14
Dioctadecyldimethylammonium	Montmorillonite, 880	2.51
Dioctadecyldimethylammonium	Montmorillonite, 680	2.45
Trioctadecylmethylammonium	Montmorillonite, 880	3.42
Trioctadecylmethylammonium	Montmorillonite, 680	3.29
Benzylhexadecyldimethylammonium	Montmorillonite, 880	1.88
Benzylhexadecyldimethylammonium	Montmorillonite, 680	1.85
Docosyltriethylammonium	Montmorillonite, 880	1.93
Decylmethyloctadecylimidazolium	Montmorillonite, 880	2.24
Didocyldimethylammonium/ dioctadecyldimethylammonium	Montmorillonite, 880	2.28
Didocyldimethylammonium/ dioctadecyldimethylammonium	Montmorillonite, 680	2.27
Benzylhydroxyethylmethyloctadecyl ammonium	Montmorillonite, 880	2.06
Benzldibutylhydroxyethylammonium	Montmorillonite, 880	1.52
Benzyldi(hydroxyethyl)butyl ammonium	Montmorillonite, 880	1.50
Benzyltriethanolammonium	Montmorillonite, 880	1.52
Benzylhydroxyethylmethyloctadecyl ammonium	Vermiculite, 1400	3.40
Benzylhexadecyldimethylammonium	Vermiculite, 1400	3.25

Reproduced from Ref. [14].

the polymer and surface modification [8]. The oxygen permeation through polyurethane nanocomposites has been described in Figure 1.4a. Interestingly, the permeation decreasing with increasing filler fraction for two of the surface modified fillers, whereas it increased with the filler fraction for one of the modified fillers. The filers for which the permeation decreased in the composites had polar modifications with better match of polarity with the polyurethane matrix. Even the

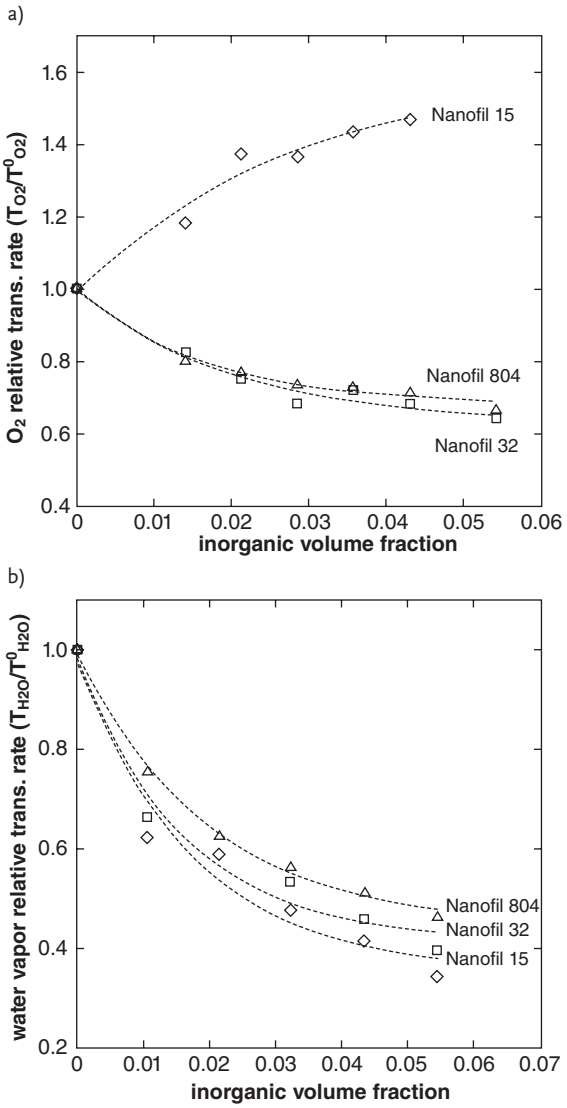

Figure 1.4 (a) Oxygen and (b) water vapor permeation through polyurethane composites. Reproduced from Ref. [8] with permission from American Chemical Society.

reactive groups present in one of the modifications were expected to chemically react with the polyurethane matrix thus leading to chemical tethering of the polymer chains on the filler surface. On the other hand, the filler for which the permeation increased through the composite had a nonpolar surface modification. This nonpolar modification had polarity mismatch with the polyurethane polymer matrix leading to the increase of interfacial voids or free volume that helped to

increase the permeation as the extent of filler increased in the composite. Another interesting observation was the behavior of water vapor transmission through the same polyurethane nanocomposites as shown in Figure 1.4b [8]. Here the permeation decreased for all the composites irrespective of the filler modification. This was a result of different interactions the permeant molecules have with the polymer matrix. Oxygen is noninteracting with the polymer matrices, whereas water molecules easily form clusters and hydrogen bonds with the polymer chains. Thus, apart from the interactions between the polymer and surface medications, specific interactions of permeant molecules with the polymer also affect the performance of nanocomposites.

Second factor affecting the properties and performance of nanocomposites is the filler volume fraction. The effect of filler volume fraction on the permeation properties of polyurethane nanocomposites has already been shown in Figure 1.4 in conjunction with the interactions between the polymer and the surface modification. Similarly, effect of filler volume fraction in conjunction with filler modification–polymer interactions is shown in Figure 1.5 for epoxy nanocomposites [9]. Two different surface modifications benzyldimethylhexadecylammonium (BzC16) and benzyldibutyl(2-hydroxyethyl) ammonium (Bz1OH) were used. Owing to the increase in the filler volume fraction, the oxygen permeation through the composites decreased. For BzC16, saturation in the permeation reduction was achieved at 4 vol% inorganic filler fraction, whereas fro Bz1OH filler, the permeation was observed to decrease further even at 5 vol% filler fraction. The performance of two fillers was significantly different from each other owing to better compatibility of the Bz1OH-modified filler with the epoxy matrix, whereas BzC16 modification had a polarity mismatch with the epoxy polymer. The permeation through the epoxy nanocomposites was also compared with the different aspect ratio fillers in Figure 1.5. In the case of BzC16 filled composites, a filler aspect ratio near to 50 was observed, whereas for the Bz1OH composites, much higher

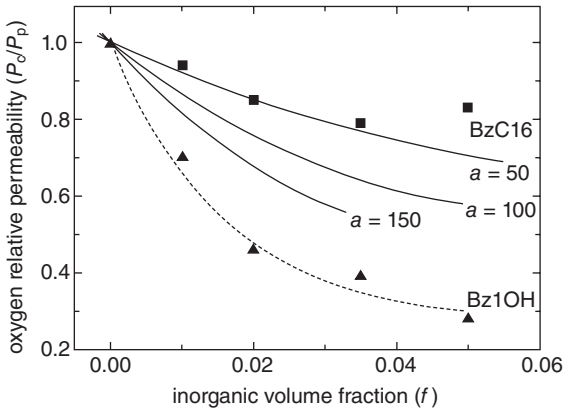

Figure 1.5 Oxygen permeation through epoxy nanocomposites as a function of filler volume fraction in the composites. Reproduced from Ref. [9] with permission from American Chemical Society.

aspect ratio of the filler was observe indicating that aspect ratio of the filler plays a significant role in defining the performance of the nanocomposites.

Apart from aspect ratio, the filler alignment or orientation is also important for certain properties of nanocomposites such as gas barrier properties. The aligned filler would provide a better resistance to the flow of the permeant molecules through the polymer matrix owing to the generation of higher extent of tortuity in the mean free path of the permeant molecules. However, in general, in most of the cases, the filler is completely misaligned in the generated composites. Apart from misalignment, the filler platelets are also observed to be bent and folded. Figure 1.6 presents one such example of polyurethane nanocomposites [8]. The filler platelets are observed to be both intercalated and exfoliated. The orientation or alignment is totally absent and the bending and folding of the platelets is clearly observed. Figure 1.7 also shows the impact of the misaligned filler on the barrier properties in comparison with the aligned filler. Figure 1.7a is the theoretical model depicting the actual misaligned filer in the composites and Figure 1.7b shows the predictions based on the model [17]. At an aspect ratio of 150 or higher, the misaligned filler was observed to be only one-third effective in generating permeation resistance as compared to the aligned filler.

Synthesis methodology is another factor affecting the microstructure and properties of polymer nanocomposites. There are different methods available to manufacture polymer nanocomposites and have their own advantages and limitations. These are detailed in Section 1.2.

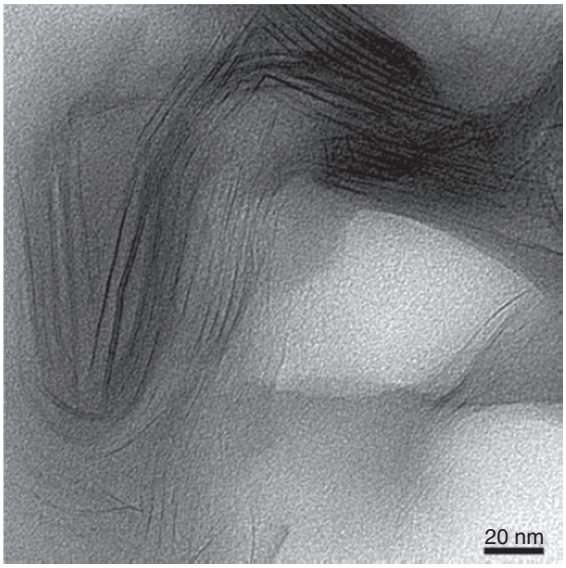

Figure 1.6 TEM micrograph of a PU nanocomposite indicating complete misalignment of the filler platelets. Reproduced from reference [8] with permission from American Chemical Society.

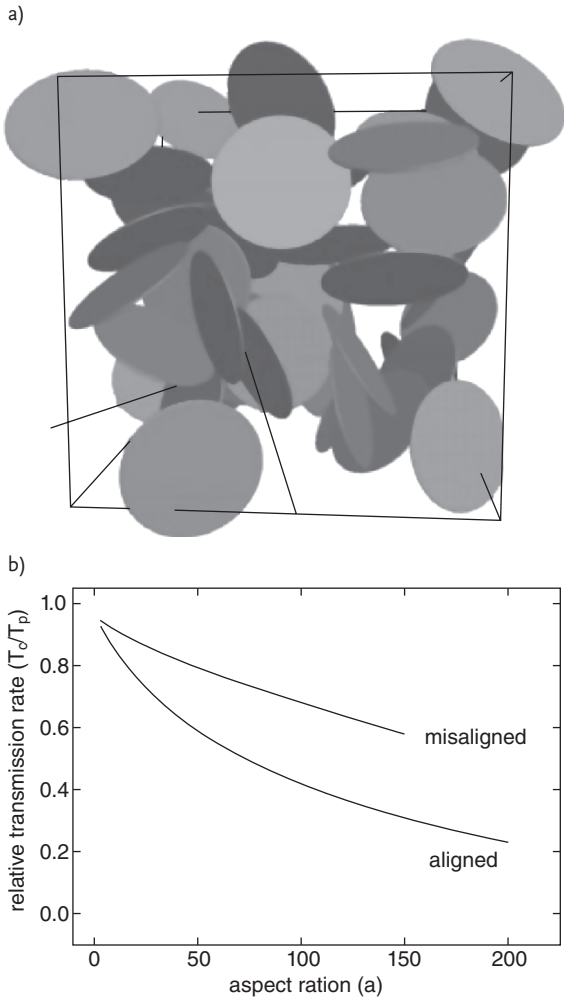

Figure 1.7 (a) Theoretical model showing the complete misalignment of filler platelets and (b) influence of filler misalignment on permeation properties. Reproduced from Ref. [17] with permission from Wiley.

1.2 Synthesis Methods

There are four general methods for the nanocomposite synthesis:

1) template synthesis
2) intercalation of polymer from solution
3) melt intercalation
4) *in-situ* synthesis.

Template synthesis involves the synthesis of inorganic material in the presence of polymer matrix. Double-layer hydroxide-based nanocomposites have been synthesized by using this route [18, 19]. The polymer aids the nucleation and growth of the inorganic host crystals and gets trapped within the layers as they grow. Template synthesis technique is not widely used even though it presents potential to generate exfoliated nanocomposites. Drawbacks like use of high temperature and tendency of the generated filler to aggregate are also to be considered.

In intercalation of polymer from solution mode of nanocomposite synthesis, the organically modified silicate is dispersed in a solvent in which the polymer is also soluble. The polymer then adsorbs onto the delaminated sheets followed by the evaporation of the solvent. When the solvent is evaporated, the sheets reassemble, which also trap the polymer chains in between. Thus, an ordered multilayer structure is usually formed using this approach. The polymer chains loose entropy in the process of intercalation, which is compensated by the increase in the entropy of the solvent molecules due to their desorption from the filler interlayers. The technique is mostly used for the intercalation of the water-soluble polymers like poly(vinyl alcohol), poly(ethylene oxide), poly(acrylic acid), poly(vinlypyrrolidone), etc. [20–24]. Later on, the use of this technique was also undertaken in organic solvents for polymers nonsoluble in water [25, 26].

Melt intercalation is one of the most commonly used techniques for the synthesis of polymer nanocomposites [27–30]. The high molecular weight polymer is melted at high temperature and the filler is then blended with the polymer melt at high temperature under shear. Thus, this mode of composite generation does not require any chemical synthesis or solvent. But the intercalation of high molecular weight polymer chains in the filler interlayers is still a challenge as both thermodynamic and kinetic factors influence the intercalation. Therefore, it is essential to modify the filler in a way that it can be exfoliated in the polymer matrix by the action of shear. In contrast, low molecular weight compatibilizers can also be added to compatibilize both the organic and inorganic components so as to enhance polymer intercalation. Figure 1.8 shows one such example of melt intercalation method, in which modified filler was first mixed with low molecular weight compatibilizer, followed by the compounding of this hybrid with high molecular weight matrix polymer [27]. As melt intercalation method uses high temperature for mixing of the organic and inorganic components, therefore, thermal degradation of the filler modification and polymer poses a concern. As even a small extent of degradation can alter the filler matrix interactions and hence affecting the microstructure of the composites, therefore, thermal degradation needs to be avoided.

In-situ intercalation method was reported by Toyota researchers for the synthesis of polyamide nanocomposites that led to the exponential growth in the nanocomposites research. For generation of polymer nanocomposites by this method, the layered silicate mineral is swollen in monomer. After swelling, the polymerization of the monomer is initiated. As monomer is present in and out of the filler interlayers, therefore, the generated structure is exfoliated or significantly intercalated. As the rate or mechanism of polymerization in and out of the filler interlayers

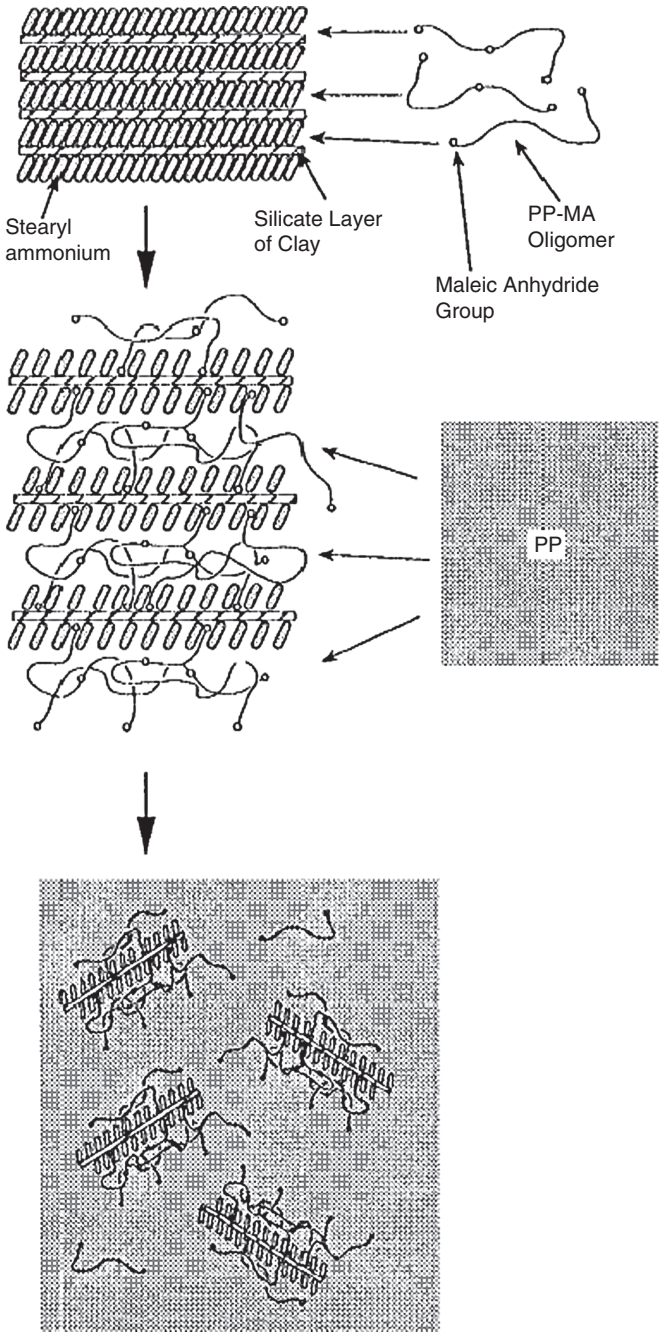

Figure 1.8 Schematic of polymer intercalation in the silicates using melt mixing approach. Reproduced from Ref. [27] with permission from American Chemical Society.

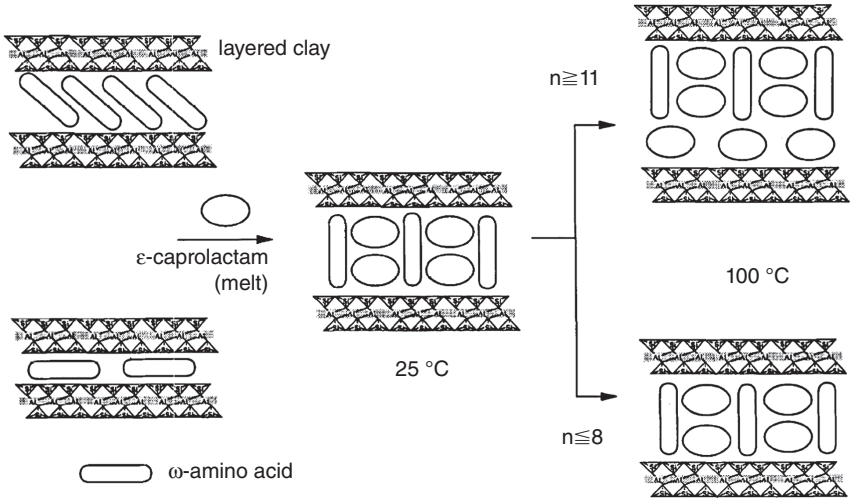

Figure 1.9 Intercalation of the modified montmorillonite with caprolactam. Reproduced from Ref. [31] with permission from Elsevier.

may be different, therefore, it is important to control there intragallery and extragallery polymerization reactions for uniform polymerization. Toyota researchers reported the modification of the montmorillonite with amino acids of different chain lengths which were subsequently swollen by caprolactam. The schematic of such a process has been demonstrated in Figure 1.9 [31]. Since then, a large number of polymers have been synthesized *in situ* in the presence of filler. Section 1.3 provides a brief overview of these systems.

1.3 *In-situ* Synthesis of Polymer Nanocomposites

In the *in-situ* synthesis approach shown in Figure 1.9, caprolactam was used to swell the filler, which was modified with amino acids of different chain lengths. The chain length of the modification had a significant effect on the extent of filler swelling as higher chain lengths led to higher extent of monomer intercalation of the filler. Figure 1.10 also shows the X-ray diffractograms of the filler modified with modifications of different chain lengths [31]. In a typical synthesis step, filler modified with 12-aminolauric acid (ALA) was swollen with caprolactam. The slurry was then heated at 250–270 °C for 48 h to polymerize caprolactam (ring-opening polymerization). The morphology of the generated composites was characterized using XRD and TEM, and it was observed that exfoliated nanocomposites were obtained when the filler content in the composite was less than 15 wt%. On the contrary, when the filler content was increased from 15 wt%, intercalated nanocomposites were obtained.

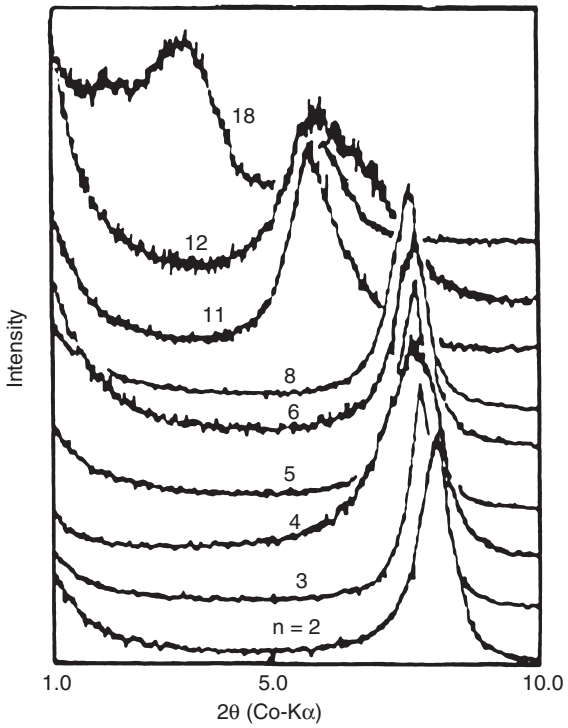

Figure 1.10 X-ray diffractograms the surface modified filler with modifications of different chain lengths; *n* corresponds to the number of carbon atoms in the modification. Reproduced from Ref. [31] with permission from Elsevier.

Nylon 12 nanocomposites were also reported following the *in-situ* synthesis approach [32]. ALA was used as both the layered silicate modifier and the monomer. Cation exchange at the filler surface by protonated ALA at low ALA concentration was observed. Further swelling of the filler with zwitterionic ALA was observed when the ALA concentration was high as shown in Figure 1.11. The swelling was observed to be independent of the temperature used for swelling, the concentration of the filler, and the type of acid used to protonate ALA. The composites morphology was partially exfoliated and intercalated.

A number of other thermoplastic and thermosetting polymer systems have been employed to generate the polymer nanocomposites using *in-situ* synthesis approach. In one such example of polyurethane nanocomposites, the modified fillers were first swollen be solvent solution of prepolymer [8]. To this mixture was then added a crosslinker followed by polymerization and evaporation of solvent. The generated nanocomposites had exfoliated and intercalated morphology depending on the chemical architecture of the surface modifications. The modification that had polymer groups such as OH groups had much better compatibility with the polymer matrix which led to the extensive exfoliation of the filler in the

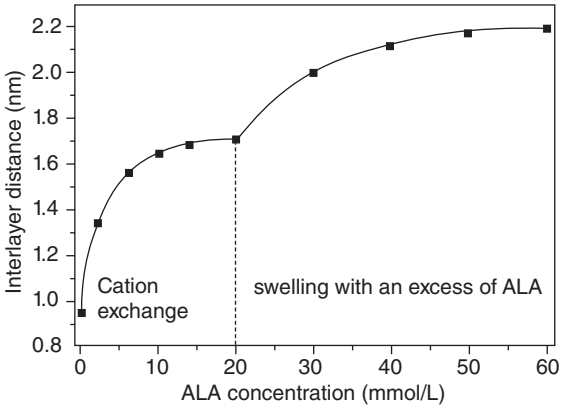

Figure 1.11 Interlayer distance in the modified filler as a function of the ALA concentration. Reproduced from Ref. [32] with permission from Wiley.

Figure 1.12 TEM micrograph of polyurethane nanocomposite containing filler modified with bis(2-hydroxyethyl) hydrogenated tallow ammonium. Reproduced from Ref. [8] with permission from American Chemical Society.

composite. Figure 1.12 shows the TEM micrograph of such nanocomposite containing filler modified with bis(2-hydroxyethyl) hydrogenated tallow ammonium. The potential reaction of OH groups in the surface modification with the polymer thus leading to the chemical tethering of the polymer chains on the filler surface helps further to exfoliate the filler. On the other hand, for other modifications that

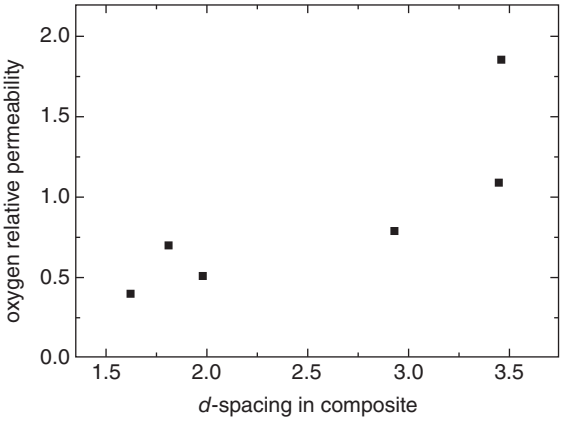

Figure 1.13 Correlation between the relative oxygen permeability through the composites with filler basal plane spacing in the composite. Reproduced from Ref. [9] with permission from American Chemical Society.

did not have any polar groups such as dimethyl dihydrogenated tallow ammonium led to the generation of only intercalated nanocomposites.

In another example of epoxy nanocomposites [9], a number of surface modifications differing in chemical architecture were used to modify the filler. Similar to the polyurethane nanocomposites, the modified fillers with better polarity match with the epoxy polymer were more exfoliated than intercalated, whereas for all other modified fillers, only intercalated morphology of the composite was obtained. The influence of intercalated and exfoliated filler on the composite properties was also demonstrated as shown in Figure 1.13. The oxygen permeation properties were plotted as a function of filler basal plane spacing in the composite. The oxygen permeation through the composites was observed to roughly increase on increasing the basal plane spacing of the filler, which is contrary to the expectation. Therefore, it signified no correlation between the oxygen permeation properties and the filler intercalation. In other words, it is not the intercalated filler, but the exfoliated filler, which enhances the composite properties. Thus, only intercalation of polymer in the filler interlayer is not enough to enhance the composite properties significantly, the filler needs to be significantly exfoliated. In the case of exfoliated nanocomposites, impressive reduction in oxygen permeation was observed.

Messersmith and Giannelis [33] reported the synthesis of epoxy nanocomposites by using *in-situ* synthesis approach. They used different curing agents and curing conditions for the generation of nanocomposites. The authors studied the swelling of the modified filler with the epoxy prepolymer. Montmorillonite modified with bis(2-hydroxyethyl)methyl halogenated tallow ammonium was observed to be readily dispersible in diglycidyl ether of bisphenol A (DGEBA). As shown in Figure 1.14, the layer spacing increased when the filler was added with DGEBA. The increased basal spacing indicated the intercalation of the prepolymer chains in the filler interlayers. The temperature was also observed to have an impact on

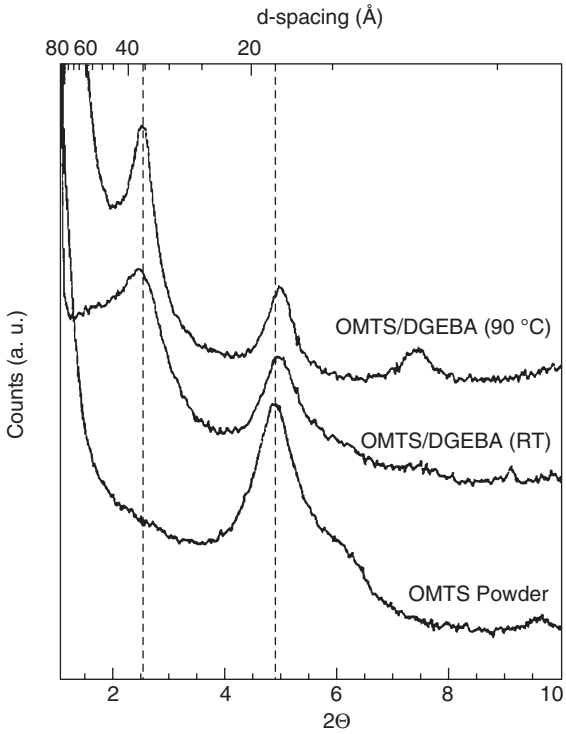

Figure 1.14 X-ray diffraction patterns of the modified filler and the mixture of epoxy prepolymer with filler at room temperature and at 90 °C. Reproduced from Ref. [33] with permission from American Chemical Society.

the extent of intercalation as it was also observed to increase when the swelling was performed at a temperature of 90 °C. Although the DGEBA prepolymer molecules intercalated the filler interlayers indicating a better polarity match between them and the filler surface, the filler platelets were still not completely delaminated as confirmed by the diffraction peak at lower angles. This was also observed in another study [9] in which the surface modifications of different chemical architectures were used and most of the modifications did not lead to the complete exfoliation of the filler platelets when the filler was swollen with epoxy prepolymer solution. Figure 1.15 also shows the XRD patterns indicating the generation of exfoliated morphology in the silicate/DGEBA/benzyldimethlyamine system as a function of temperature [33]. The scan temperature increased vertically from bottom to top of the figure. At lower temperature, complete exfoliation of the filler was not achieved and a mix of both of intercalated and unintercalated silicate platelets was present. When the temperature was increased, disappearance of the diffraction peaks occurred indicating the filler delamination during heating. The authors also observed significant influence of the nature of the curing agent on the morphology of the composites. Only intercalated nanocomposites were

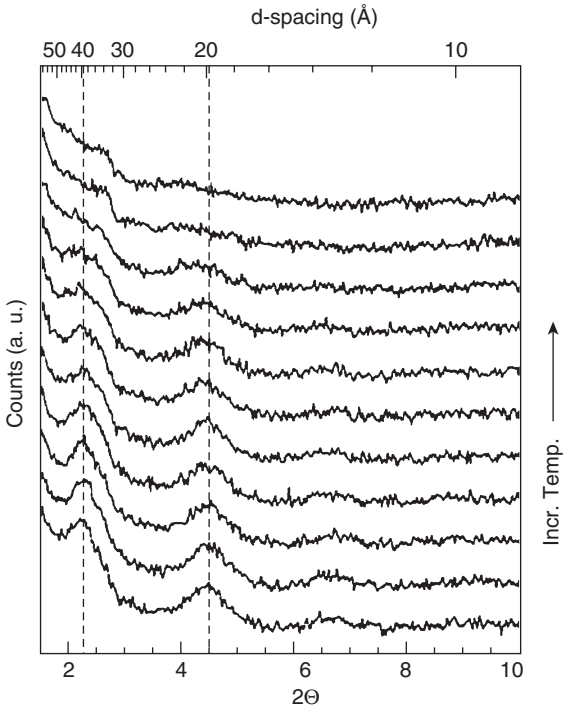

Figure 1.15 X-ray diffraction patterns of filler/DGEBA/benzyldimethlyamine system at different temperatures from 20 to 150 °C. Reproduced from Ref. [33] with permission from American Chemical Society.

obtained when using diamines as curing agents. On the contrary, when benzyldimethlyamine was used as curing agent, exfoliated nanocomposites were obtained. The bridging of silicate layers (and hence degellation) by the amine curing agent was suggested as a reason for the generation of intercalated morphology in the composites when using diamines as curing agents. Another factor contributing to such degellation is the presence of excess modification molecules on the surface of filler. These molecules can also react with the curing agent or the epoxy polymer thus disturbing the interface between the filler and polymer.

Generation of PET nanocomposites by *in-situ* synthesis of PET (direct condensation reactions of diol and diacid) in the presence of clay was not successful [34] as only low molecular weight polymer was observed due to poor control on stoichiometry. Melt intercalation method was also employed for the generation of PET nanocomposites, but only intercalated nanocomposites were observed by this method. This was owing to the kinetic hindrance to the high molecular weight polymer chains to enter the filler interlayers. As an alternative, ring-opening polymerization of ethylene terepthalate cyclic oligomers in the presence of organically modified montmorillonites was used. The schematic of the process leading to generation of PET nanocomposites is depicted in Figure 1.16. The filler interlayers

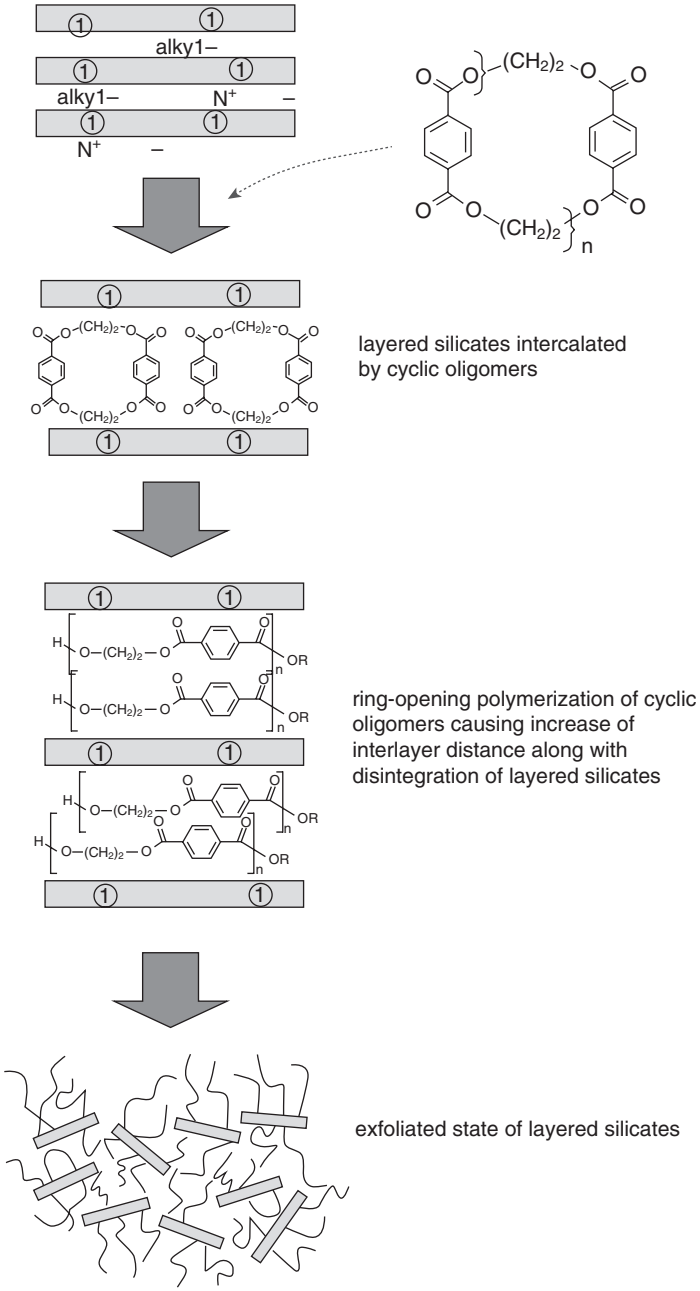

Figure 1.16 Ring-opening polymerization of cyclic oligomers to generate PET nanocomposites. Reproduced from Ref. [34] by permission from Elsevier.

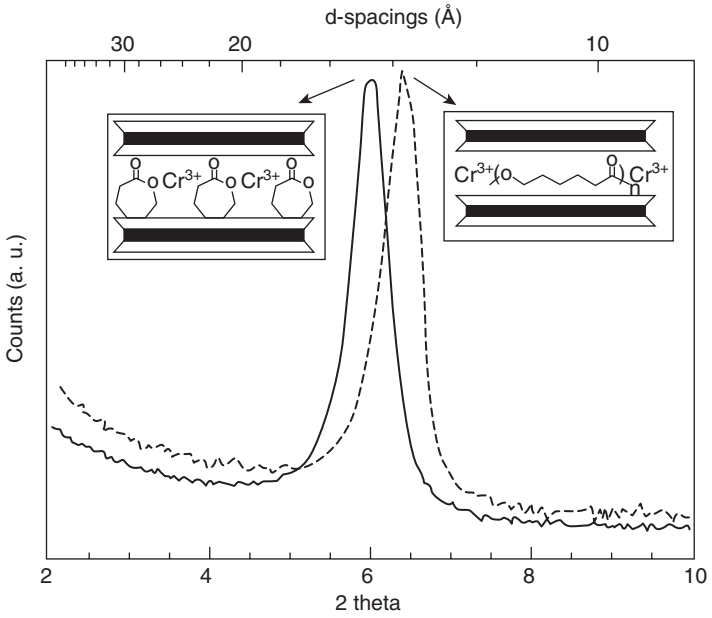

Figure 1.17 X-ray diffraction patterns of the intercalated filler (solid line) and the nanocomposite material (dashed line). Reproduced from Ref. [35] with permission from American Chemical Society.

were swollen with cyclic oligomers. These cyclic oligomers owing to their low molecular weight and hence lower viscosity could easily intercalate in the filler interlayers. Ring-opening polymerization of the oligomers led to further increase in the interlayer distance followed by filler delamination.

In-situ synthesis of caprolactone in the interlayers of Cr^{3+}-modified fluorohectorite was reported by Messersmith *et al.* [35]. The microstructure development was studied by using XRD as shown in Figure 1.17. The unintecalated filler had a basal plane spacing of 12.8 Å, which was increased to 14.6 Å for the intercalated filler swollen with caprolactone. After the polymerization of caprolactone in and around of filler interlayers, a final basal plane spacing of 13.7 Å was observed for the nanocomposite. The observed basal plane spacing correlated well with 4-Å interchain distance in the crystal structure of poly(caprolactone).

Polyolefin nanocomposites have also been reported by using gas phase by *in-situ* polymerization [36, 37]. In this technique, a Zieler–Natta or any other coordination catalyst is anchored to the surface of the layered silicates. The anchoring of the catalyst is not achieved by the usual cation exchange, but it is achieved by the electrostatic interactions of the catalytic materials with MAO initially anchored to the filler surface. The molecular weight of the generated polymer can also be controlled by the addition of chain transfer agent. It was also observed by the authors that in the absence of chain transfer agent, molecular weight of the polymer was too high to proceed further and hydrogen was added to improve

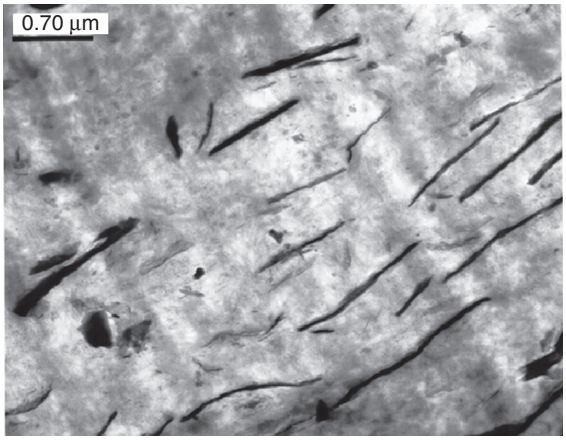

Figure 1.18 TEM micrograph of the polyethylene nanocomposites prepared by *in-situ* polymerization. Reproduced from Ref. [37] with permission from Elsevier.

the processability [36]. Figure 1.18 shows the TEM micrograph of the polyethylene nanocomposites prepared by the *in-situ* polymerization approach. Good dispersion of the filler in the polymer matrix was achieved. Other studies on the *in-situ* synthesis of polyolefin naoconpoites have also been reported [38–40].

Akelah *et al*. also reported vinylbenzyltrimethylammonium-modified montmorillonites [41]. The presence of vinyl groups was helpful in copolymerizing them with an external monomer like styrene in order to chemically tether or graft the polymer chains to the filler surface. Fu and Qutubuddin also reported the synthesis of a polymerizable cationic surfactant, vinylbenzyldimethyldodecylammonium chloride with terminal monomer moiety [42]. The surfactant was ion exchanged on the clay surface and the modified clay was swollen with styrene monomer. Free radical polymerization of styrene with azo bis(iso-butyronitrile) as initiator led to the generation of exfoliated polystyrene–clay nanocomposites. Mittal [43] also reported the partial exchange of filler surface with methacryloxyethyltrimethylammonium chloride and the remaining surface with nonreactive modification as shown in Figure 1.19. The free radical polymerization of lauryl methacrylate in the presence of modified montmorillonite led to the tethering of poly(lauryl methacrylate) chains to the filler surface. The successful grafting was confirmed with increased organic weight loss in thermogravimetric analysis and increased basal plane spacing in XRD.

Living or controlled polymerization techniques have also been frequently used for the *in-situ* synthesis of polymer nanocomposites. Figure 1.20 shows the example of styrene polymerization in the presence of modified filler. The filler modification consisted of ammonium cation bearing a notroxide moiety [44]. Styrene was polymerized in bulk at 125 °C for 8 h. No diffraction peaks were observed in the XRD confirming extensive exfoliation of the filler. TEM micrographs also confirmed the uniform distribution of filler in the matrix. Generation

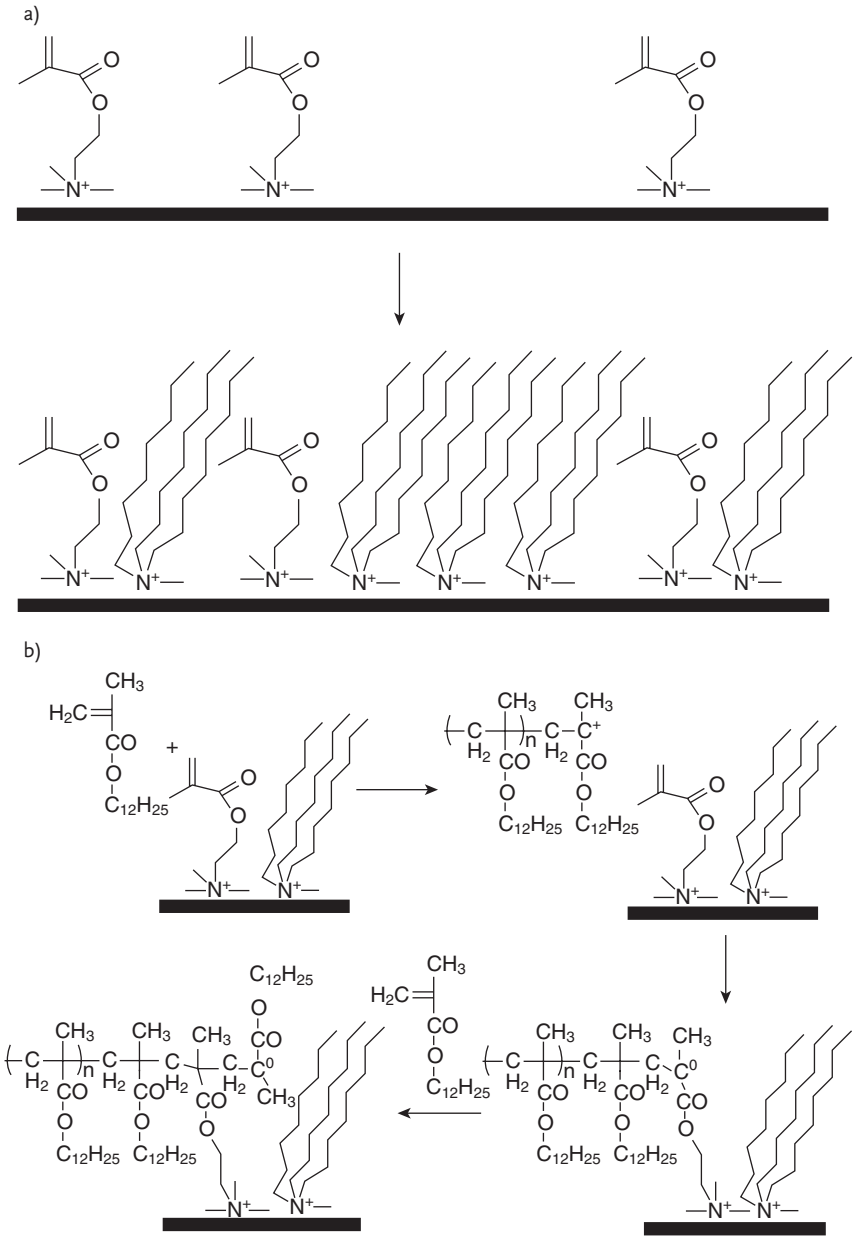

Figure 1.19 (a) Schematic of surface modification and (b) schematic of lauryl methacrylate polymerization on the filler surface. Reproduced from Ref. [43] with permission from Elsevier.

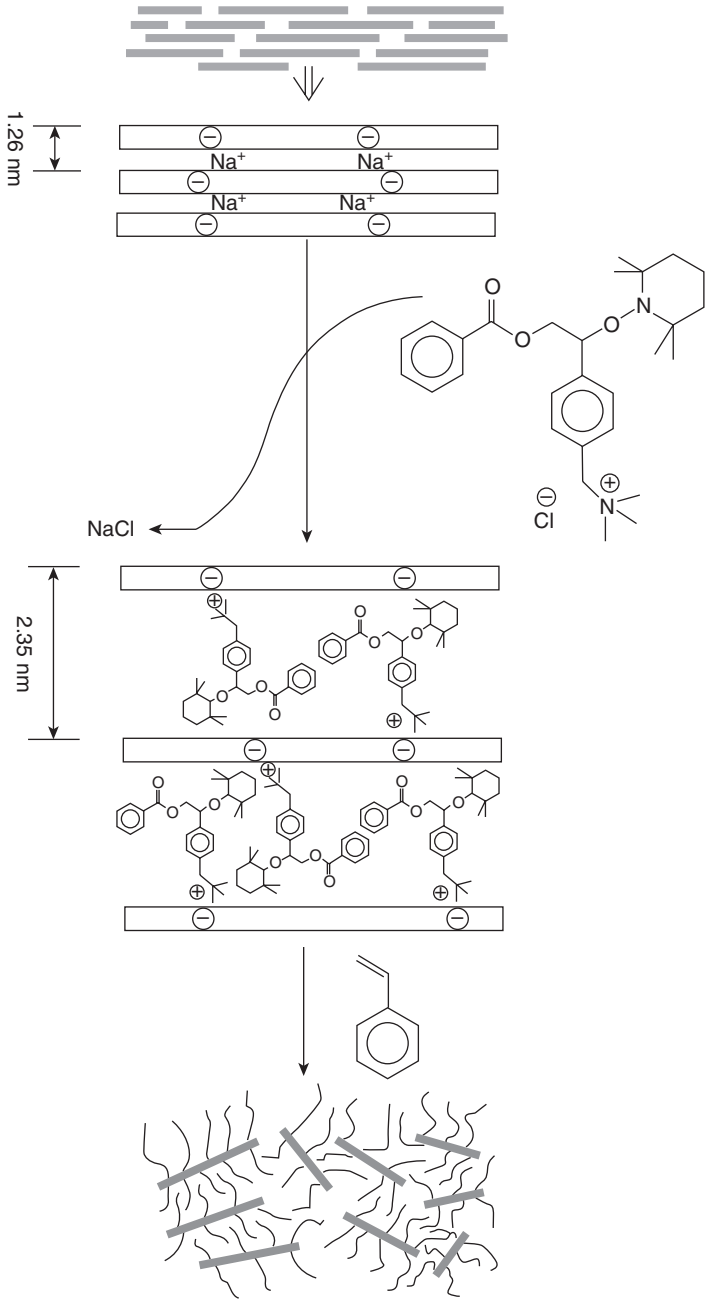

Figure 1.20 Schematic of the nitroxyl-based organic cation modification of montmorillonite surface and generation of PS nanocomposite. Reproduced from Ref. [44] with permission from American Chemical Society.

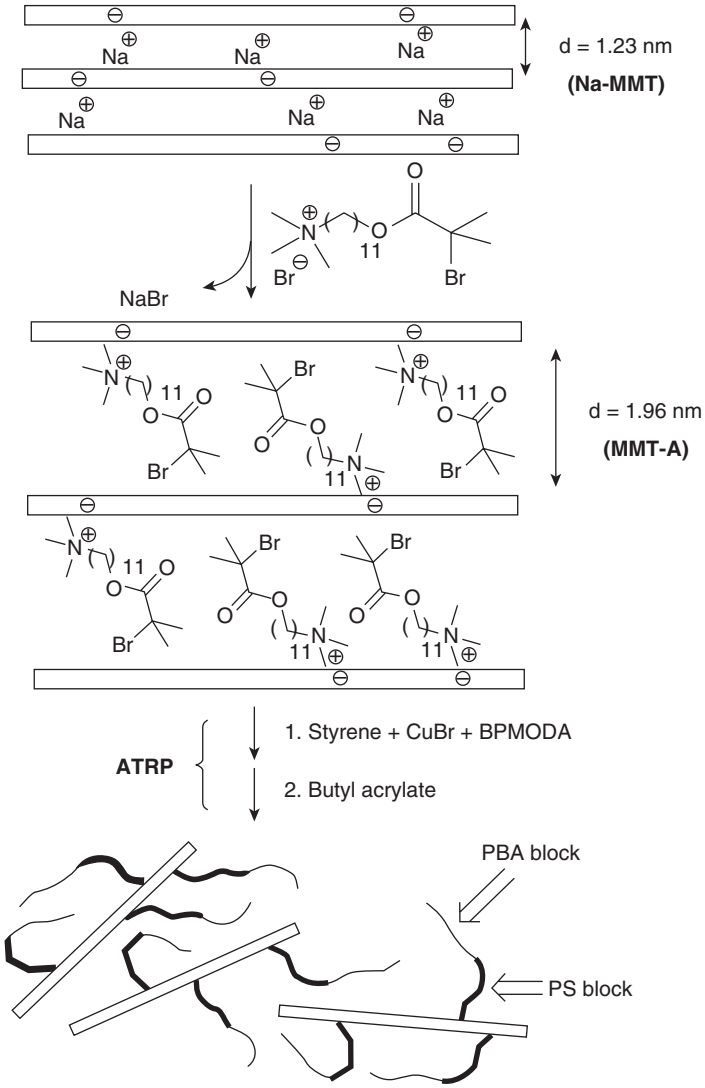

Figure 1.21 Nanocomposites based on block copolymer generated by atom transfer radical polymerization. Reproduced from Ref. [45] by permission from Elsevier.

of block copolymer of poly(styrene-block-butylacrylate) grafted from the clay surface by using ATRP approach was also reported by Zhao *et al.* [45]. Styrene was polymerized first followed by polymerization of butyl acrylate. Figure 1.21 shows the schematic of the process. The ATRP initiator had a terminal ammonium moiety that was used for ion exchange on the filler surface.

References

1 Yano, K., Usuki, A., Okada, A., Kurauchi, T., and Kamigaito, O. (1993) *J. Polym. Sci., Part A: Polym. Chem.*, **31**, 2493.
2 Kojima, Y., Fukumori, K., Usuki, A., Okada, A., and Kurauchi, T. (1993) *J. Mater. Sci. Lett.*, **12**, 889.
3 Vaia, R.A., Ishii, H., and Giannelis, E.P. (1993) *Chem. Mater.*, **5**, 1694.
4 Mehrotra, V. and Giannelis, E.P. (1990) *Mater. Res. Soc. Symp. Proc.*, **171**, 39.
5 Bailey, S.W. (1984) *Reviews in Mineralogy*, Virginia Polytechnic Institute and State University, Blacksburg, VA, USA.
6 Brindley, G.W. and Brown, G. (1980). *Crystal Structures of Clay Minerals and Their X-Ray Identification* (eds G.W. Brindley and G. Brown), Mineralogical Society, London, UK.
7 Vaia, R.A., Teukolsky, R.K., and Giannelis, E.P. (1994) *Chem. Mater.*, **6**, 1017.
8 Osman, M.A., Mittal, V., Mobridelli, M., and Suter, U.W. (2003) *Macromolecules*, **36**, 9851.
9 Osman, M.A., Mittal, V., Mobridelli, M., and Suter, U.W. (2004) *Macromolecules*, **37**, 7250.
10 Osman, M.A., Mittal, V., and Suter, U.W. (2007) *Macromol. Chem. Phys.*, **208**, 68.
11 Mittal, V. (2007) *J. Thermoplastic Comp. Mater.*, **20**, 575.
12 Osman, M.A., Rupp, J.E.P., and Suter, U.W. (2005) *J. Mater. Chem.*, **15**, 1298.
13 Mittal, V. (2009) *J. Thermoplastic Comp. Mater.*, **22**, 453.
14 Mittal, V. (2010). *Advances in Polymer Nanocomposites Technology* (ed. V. Mittal), Nova Science Publishers, New York.
15 Mittal, V. (2009). *Optimization of Polymer Nanocomposite Properties* (ed. V. Mittal), Wiley-VCH Verlag GmbH, Weinheim.
16 Beyer, G. (2002) *Plast. Addit. Compound.*, **4**, 22.
17 Osman, M.A., Mittal, V., and Lusti, H.R. (2004) *Macromol. Rapid Commun.*, **25**, 1145.
18 Wilson, O.C., Jr., Olorunyolemi, T., Jaworski, A., Borum, L., Young, D., Siriwat, A., Dickens, E., Oriakhi, E., and Lerner, M. (1999) *Appl. Clay Sci.*, **15**, 265.
19 Oriakhi, C.O., Farr, I.V., and Lerner, M.M. (1997) *Clays Clay Miner.*, **45**, 194.
20 Ruiz-Hitzky, E., Aranda, P., Casal, B., and Galvan, J.C. (1995) *Adv. Mater.*, **7**, 180.
21 Ogata, N., Kawakage, S., and Ogihara, T. (1997) *J. Appl. Polym. Sci.*, **66**, 573.
22 Parfitt, R.L. and Greenland, D.J. (1970) *Clay Miner.*, **8**, 305.
23 Billingham, J., Breen, C., and Yarwood, J. (1997) *Vib. Spectrosc.*, **14**, 19.
24 Levy, R. and Francis, C.W. (1975) *J. Colloid Interface Sci.*, **50**, 442.
25 Jeon, H.G., Jung, H.-T., Lee, S.W., and Hudson, S.D. (1998) *Polym. Bull.*, **41**, 107.
26 Krikorian, V. and Pochan, D. (2003) *Chem. Mater.*, **15**, 4317.
27 Kawasumi, M., Hasegawa, N., Kato, M., Usuki, A., and Okada, A. (1997) *Macromolecules*, **30**, 6333.
28 Fornes, T.D., Yoon, P.J., Keskkula, H., and Paul, D.R. (2001) *Polymer*, **42**, 9929.
29 McNally, T., Murphy, W.R., Lew, C.Y., Turner, R.J., and Brennan, G.P. (2003) *Polymer*, **44**, 2761.
30 Davis, C.H., Mathias, L.J., Gilman, J.W., Schiraldi, D.A., Shields, J.R., Trulove, P., Sutto, T.E., and Delong, H.C. (2002) *J. Polym. Sci., Part B: Polym. Phys.*, **40**, 2661.
31 Okada, A. and Usuki, A. (1995) *Mater. Sci. Eng.*, **C3**, 109.
32 Reichert, P., Kressler, J., Thomann, R., Mulhaupt, R., and Stoppelmann, G. (1998) *Acta Polym.*, **49**, 116.
33 Messersmith, P.B. and Giannelis, E.P. (1994) *Chem. Mater.*, **6**, 1719.
34 Lee, S.-S., Ma, Y.T., Rhee, H.-W., and Kim, J. (2005) *Polymer*, **46**, 2201.
35 Messersmith, P.B. and Giannelis, E.P. (1993) *Chem. Mater.*, **5**, 1064.
36 Dubois, P., Alexandre, M., Hindryckx, F., and Jerome, R. (1998) *J. Macromol. Sci. Rev. Macromol. Chem. Phys.*, **C38**, 511.
37 Alexandre, M., Dubois, P., Sun, T., Garces, J.M., and Jerome, R. (2002) *Polymer*, **43**, 2123.
38 Bergman, J.S., Chen, H., Giannelis, E.P., Thomas, M.G., and Coates, G.W. (1999) *J. Chem. Soc. Chem. Commun.*, **21**, 2179.

39 Jin, Y.-H., Park, H.-J., Im, S.-S., Kwak, S.-Y., and Kwak, S. (2002) *Macromol. Rapid Commun.*, **23**, 135.
40 Heinemann, J., Reichert, P., Thomann, R., and Muelhaupt, R. (1999) *Macromol. Rapid Commun.*, **20**, 423.
41 Akelah, A. and Moet, A. (1996) *J. Mater. Sci.*, **31**, 3589.
42 Fu, X. and Qutubuddin, S. (2001) *Polymer*, **42**, 807.
43 Mittal, V. (2007) *J. Colloid Interface Sci.*, **314**, 141.
44 Weimer, M.W., Chen, H., Giannelis, E.P., and Sogah, D.Y. (1999) *J. Am. Chem. Soc.*, **121**, 1615.
45 Zhao, H., Farrell, B.P., and Shipp, D.A. (2004) *Polymer*, **45**, 4473.